Journal of Applied Fluid Mechanics , Vol. 9, No. 3, pp. 1421-1435, 2016.
Available online at www.jafmonline.net, ISSN 1735-3572, EISSN 1735-3645.
DOI: 10.18869/acadpub.jafm.68.228.24178

LES of Flow past Circular Cylinder at $Re = 3900$

B. N. Rajani †,[1] A. Kandasamy[2] and Sekhar Majumdar[3]

[1] *CTFD Division, National Aerospace Laboratories(CSIR), Bangalore, 560 017 India*
[2] *DMACS, National Institute of Technology Karnataka, Surathkal 575 025, India*
[3] *Dept. of Mech. Engg., NITTE Meenakshi Institute of Technology, Bangalore 560 640, India*

† *Corresponding Author Email*: *rajani@ctfd.cmmacs.ernet.in*

(Received November 3, 2014; accepted April 15, 2015)

ABSTRACT

Transitional flow past a circular cylinder in the lower subcritical regime ($Re = 3900$) has been analysed using Large Eddy Simulation (LES) coupled to Smagorinsky and dynamic sub grid scale models. These simulations have been carried out using a parallel multiblock structured finite volume code which is based on SIMPLE algorithm. The predictions are validated against detailed measurement data for mean as well as turbulence quantities. The present LES prediction in general agree reasonably well with the measurement data in the near wake region but deviates from the measurement data in the far wake region which may be due to the coarse resolution of the grid in this region. The influence of the SGS model on mean flow quantities as well as on the flow structures are also discussed.

Keywords: LES; Implicit finite volume solver; Smagorinsky and dynamic SGS model.

NOMENCLATURE

C	dynamic coefficient
C_d	total drag coefficient
C_f	non-dimensional skin friction coefficient
C_p	non-dimensional pressure coefficient
C_{pb}	base pressure
C_s	smagorinsky
D	cylinder diameter
f_w	van Driest damping function
J	Jacobian of the transformation matrix
N_c	no. of averaging cycle
N_z	no. of nodes along the span
$\overline{P}$	grid filtered (resolved) pressure
Re	flow Reynolds number based on D
$\mid S \mid$	strain rate tensor
St	Strouhal number
$\overline{U_i}$	grid filtered velocity components along i-direction
U_∞	freestream velocity
y^+	non-dimensional wall normal distance
U_{CL}	centerline streamwise velocity
ρ	density
μ	fluid viscosity
μ_{sgs}	SGS eddy viscosity
η_k^i	metric coefficients of transformation
θ	circumferential angle of the cylinder
θ_{sep}	flow separation angle on the cylinder surface
$\overline{\Delta_i}$	grid size in the i-direction
$\widehat{\Delta}$	test filter
$\Delta\bar{t}$	non-dimensional time step size
min	minimum
sep	separation
CCDS	compact central difference scheme
CDS	central difference scheme
CFD	computational fluid dynamics
CR	coarse resolution
DES	detached eddy simulation
DM	dynamic global-coefficient SGS model of Park *et al.* (2006)
DM1	dynamic global-coefficient SGS model of You and Moin (2006)
DNS	direct numerical simulation
DSM	dynamic subgrid scale model of Germano *et al.* (1991)
FES	finite element spectral
FVFEC	finite volume finite element mixture solver for compressible flows
HR	high resolution

IBM	immersed boundary method
LES	large eddy simulation
MUSCL	monotone upwind scheme for conservation laws
NS	navier stokes
PIV	particle image velocimetry
SFM	structure function model
SGS	subgrid scale
SSM	smagorinsky subgrid scale model with van driest damping function
SSMP	smagorinsky subgrid scale model with panton damping function
Tetra	tetrahedral
URANS	unsteady reynolds averaged navier stokes
UG	unstructured grid
VMS	variational multiscale
WALE	wall adapting local eddy viscosity

1. INTRODUCTION

Flow past circular cylinder is a classic example of unsteady three-dimensional flow consisting of separation, reattachment, free shear layer instabilities due to three dimensional disturbances and transition from laminar to turbulent state of flow in the wake of the cylinder. In spite of extensive experimental and numerical studies (Beaudan and Moin 1994; Norberg 1987), flow around a circular cylinder still remains a challenging problem in fluid mechanics leading to a continuous investigations to understand the complex unsteady dynamics of the cylinder flow. Both measurements and computations for flow past circular cylinder over a wide range of Reynolds number, have revealed distinct flow patterns which have later been classified (Roshko 1954; Williamson 1996; Zdravkovich 1997) into different flow regimes. The flow remains steady and laminar for Reynolds number between 5 and 47 and the wake starts becoming unstable at a critical Reynolds number around 47, leading to the shedding of alternate vortices from the cylinder surface at definite frequencies, well known as the von Karman vortex street. The laminar vortex shedding is observed to be continuing up to a value of Re of about 190, beyond which the two-dimensional flow becomes unstable which leads to the formation and amplification of three-dimensional instabilities in the far wake region (Zhang *et al.* 1995; Williamson 1996; Thompson *et al.* 1996; Mittal and Balachandra 1997; Mittal 2001; Rajani *et al.* 2009). These three dimensional disturbance leads to the simultaneous formation of spanwise and streamwise vortex structure along the spanwise direction and the far wake zone undergoes transition from laminar to turbulent state. The flow at $Re = 3900$ falls under the lower subcritical range of flow where the flow remains laminar beyond separation and transition takes place in the free shear layer in the wake. In this flow regime, the transition waves appear along the free shear layer and the turbulent eddies are shed periodically along the wake of the cylinder. The simultaneous presence of different scales makes numerical simulation of this flow very difficult. The widely used URANS approach with eddy viscosity based turbulence models are usually found (Deng *et al.* 1993; Cox 1997; Rajani *et al.* 2012) to be inaccurate and unreliable for transitional flow. The DNS provides a reliable and valuable information on the all flow physics of this transitional flow, but the computational cost is prohibitively high even at a relatively low Reynolds number. The LES approach, on the other hand, is a kind of compromise between the DNS and the URANS approach. In the LES approach, the NS equations are first filtered spatially to identify the resolved flow variables representing large scale motion for which direct simulation is used and the interaction term between the resolved and the unresolved flow variables are simulated through the SGS models. The present paper focuses on the numerical solution of flow past a circular cylinder at $Re = 3900$ using LES coupled to the Smagorinsky and Dynamic SGS models and the computational results are validated against detailed measurement data (Norberg 1987; Lourenco and Shih 1993; Ong and Wallace 1996) for the mean flow and turbulence quantities.

Several experiments and computations have been carried out for the flow past a circular cylinder at $Re = 3900$. The PIV measurement of Lourenco and Shih (1993) provide extensive data on both mean flow and turbulent quantities at several streamwise locations. The hot wire measurements of Ong and Wallace (1996) provide the mean flow quantities at several locations mainly in the near wake of the cylinder. The DNS computation of Rai *et al.* (1993) using higher order upwind schemes are in reasonable agreement with experimental data for the mean velocity and Reynolds stress profile. However some differences observed between simulation and measurement data in the recirculating region and shape of streamwise velocity profile have been attributed mostly to experimental errors. The other DNS computations have been carried out by Ma *et al.* (2000) and Dong *et al.*

(2006). Ma *et al.* (2000) performed a detailed study and observed two distinct shapes of the transverse profiles of the mean streamwise velocity in the near wake. It was further argued that the shape of these profiles depend greatly on the length and the resolution of the spanwise domain. Wissink and Rodi (2008) conducted a series of DNS of incompressible flow around a circular cylinder at $Re = 3300$ and reasonable agreement was obtained between the simulation and measurement data. In this study, the size and resolution of the computational domain has been varied in order to study its influence on the turbulence statistics. More recently Rai (2010) has used DNS inorder to investigate the phenomena of intermittency and shear layer transition. In this paper Rai (2010) has the computed time traces of the velocity and instantaneous vorticity contours to understand and explain the fundamental process of intermittency and shear layer transition.

The first large eddy simulation for flow past circular cylinder at the subcritical Reynolds number ($Re = 3900$) has been reported by Beaudan and Moin (1994). These simulations were performed using high-order upwind biased schemes on an O-grid and also established a grid-independent solution in the vicinity of the cylinder. Though their simulation demonstrates reasonable agreement with the measurement data for mean velocity profiles, the turbulent quantities at several downstream locations do not match well with the experimental data. These discrepancies observed at the downstream stations have been mainly attributed to the numerical dissipation present in the flux discretisation schemes used. Their simulation using the dynamic subgrid scale model is found to be slightly better than those obtained using either the conventional Smagorinsky model or even with no subgrid scale model. However the effect of subgrid scale model is not found to be very significant. Mittal and Moin (1997) in their work on large eddy simulation for flow past a circular cylinder at $Re = 3900$ have used a second order conservative scheme coupled to a Fourier spectral method with periodic boundary condition along the spanwise direction. Their simulation results agree reasonably well with the measurement data as well as with those obtained by the upwind-biased simulation of Beaudan and Moin (1994). The comparison of the power spectra of the velocity fluctuations show that their computation has a better agreement with the measurement data when compared to the simulation of Beaudan and Moin (1994). From these computation results, Mittal and Moin (1997) concluded that non dissipative methods are more suitable for LES. However even in spite of using non-dissipative schemes, this simulation shows a lot of discrepancies between the numerical and experimental results especially in the Reynolds stress profiles at several downstream locations and this has been attributed to the use of relatively inaccurate lower order discretisation schemes. The LES results for the same flow have been reported by Breuer (1998) using five different numerical schemes and with both the standard Smagorinsky and dynamic subgrid scale models. In this work the best agreement with the experimental data is achieved when central difference scheme is used in conjunction with the dynamic subgrid scale model. Kravchenko and Moin (2000), Blackburn and Schmidt (2001) and Franke and Frank (2002) have carried out large eddy simulations for flow past a circular cylinder at $Re = 3900$, using higher order numerical methods in order to sort out some of the issues regarding the discrepancies between hot wire measurement data and numerical simulation. Kravchenko and Moin (2000) have used a newly developed high order accurate numerical method based on B-splines to sort out the differences reported by earlier researchers (Beaudan and Moin 1994; Breuer 1998; Mittal and Moin 1997). The simulations using B-spline are found to be in better agreement with the hot-wire measurement data of Ong and Wallace (1996) especially in the far wake region (six to ten diameters downstream of the cylinder), Franke and Frank (2002) have carried out the LES of this problem in order to validate their cell-centered finite volume code that solves the compressible NS equations. They have compared their results with the DNS results of Ma *et al.* (2000) and experiments of Ong and Wallace (1996) and concluded that a larger time averaging was necessary to obtain a closer agreement. Snyder and Degrez (2003) in their paper have proposed a parallel stabilized finite-element/spectral large eddy simulation algorithm for solving two-dimensional incompressible flow. They have used the standard Smagorinsky model with van Driest damping near solid walls and have validated this algorithm for flow past circular cylinder at $Re = 3900$. Their results compare reasonably well with experimental and other numerical data for the laminar and sub critical turbulent regimes in both qualitative and quantitative sense. Park *et al.* (2006) proposed a new dynamic SGS model based on SGS eddy viscosity model proposed by Vreman (2004) to simulate turbulent flows in complex geometry using LES. This dynamic procedure determines the model coefficients by considering global equilibrium between the subgrid-scale dissipation and the viscous dissipation where the model coefficients determined are function of time only. The authors have successfully validated this new dynamic SGS model for turbulent channel flow, flow past circular cylinder at $Re = 3900$ and flow over sphere and predicted superior results compared to the fixed-coefficient Smagorinsky model. The authors claim that the proposed dynamic model is robust and can be easily applied to complex flows which have no homogenous direction. You and Moin (2006) proposed another dynamic global-coefficient SGS eddy-viscosity model which is an improvement over the SGS model proposed by Park *et al.* (2006). This dynamic procedure is also based on the global equilibrium between the SGS and viscous dissipation but requires only single level test filter in contrast to two level test filter used by Park *et al.* (2006) and hence claimed to be more suitable for complex geometries. You and Moin (2006) have also validated this new dynamic SGS model for turbulent channel flow and flow over cylinder at $Re = 3900$. Parnadeau *et al.* (2008) have carried out both experimental and numerical studies for flow at $Re = 3900$ to further sort out the previous numerical and experimental discrepancies. Ouvrard et al. (2010) have simulated flow around circular cylinder at $Re = 3900$ using unstructured grids to understand the effects of numerical viscosity and grid resolution. The simulations have been carried out using the classical LES and VMS-LES coupled to three different non-dynamic eddy viscosity based SGS models *viz.* Smagorinsky, Vreman (Vreman 2004) and WALE (Nicoud and Ducros 1999). Their study indicate that the results obtained using VMS-LES is also quite sensitive to SGS models used and does not always lead to an improved quality of prediction when compared to the classical LES. However they have recommended to use VMS-WALE which is a more general approach for predicting vortex shedding flows compared to the Smagorinsky fixed SGS model which has certain drawback at higher Reynolds number flows.

The objective of the present LES computation is mainly to assess the limitation and accuracy level of the present algorithm for computation of mean and turbulence flow quantities for flow past a circular cylinder in the lower subcritical Reynolds number. The LES algorithm coupled to SSM and DSM has been incorporated in the existing parallel multiblock flow solver 3D-PURLES (Three Dimensional Pressure based Unsteady Reynolds averaged navier-stokes and Large Eddy Simulation solver). LES computations have also been carried out without any subgrid scale model in order to study the influence of the model on the resolved scale. LES results obtained using different SGS models at $Re = 3900$ are validated against detailed hot-wire and PIV measurement data.

2. Governing Equations of Motion for LES in Physical Space

The present pressure-based finite volume algorithm for collocated variable arrangement uses a box filter as the filter kernel. The model filtered equations where the unresolved residual stress tensor appearing in the resolved momentum equations is simulated by an eddy viscosity based Subgrid Scale (SGS) model (Germano *et al.* 1991; Sagaut 1998). In the general curvilinear coordinate system with cartesian velocity component, the momentum equation for the filtered (resolved) velocity component $\overline{U_i}$ and the continuity equation are written as follows :

Mass conservation:

$$\frac{\partial}{\partial x_j}\left(\rho \overline{U_i} \eta_i^j\right) = 0 \quad (1)$$

Momentum conservation:

$$\frac{\partial\left(\rho \overline{U_k}\right)}{\partial t} + \frac{1}{J}\frac{\partial}{\partial x_j}\Big[\rho \overline{U_i}\,\overline{U_k}\eta_i^j + \overline{P}\eta_k^j - \frac{(\mu+\mu_{\mathrm{sgs}})}{J}\left(\frac{\partial \overline{U_k}}{\partial x_i}\eta_n^i\eta_n^j + \frac{\partial \overline{U_i}}{\partial x_m}\eta_i^j\eta_k^m\right)\Big] = 0 \quad (2)$$

The following two approaches are used to used to model the sub grid scale eddy viscosity, μ_{sgs}

Smagorinsky SGS model (Smagorinsky 1963) is the simplest and the widely used and is based on linear eddy viscosity hyposthesis where the μ_{sgs} is computed through the following algebraic expression based on mixing length hypothesis

$$\mu_{\mathrm{sgs}} = \rho(f_w C_s \overline{\Delta})^2 \mid \overline{S} \mid \quad (3)$$

where, $\overline{\Delta} = (\Delta_1\Delta_2\Delta_3)^{1/3}$ is the filter width, Δ_i is the grid size in the i-th direction and C_s is the Smagorinsky constant which is assumed to be 0.1 and $f_w = 1 - \exp(-y^+/25)$ is a van Driest type damping function.

Dynamic SGS model was proposed by Germano *et al.* (1991) in order to overcome some of the drawbacks of the Smagorinsky SGS model in which the eddy viscosity is defined as

$$\mu_{\mathrm{sgs}} = \rho(C\overline{\Delta})^2 \mid \overline{S} \mid \quad (4)$$

where C is not a constant but a function of time and space. In order to compute C, the present procedure uses the approach of Germano *et al.* (1991) with simplified least square contraction as suggested by Lilly (1992) and spanwise averaging as suggested by Zang *et al.* (1993), Najjar and Tafti (1996). This procedure introduces a test-filter, $\widehat{\Delta}$ which is larger than the original grid filter width ($\overline{\Delta}$). In the present study test filter is computed as $\widehat{\Delta_i} = 2\Delta_i$ as suggested by Najjar and Tafti (1996). To enhance the numerical stability, C obtained at every time step is smoothened out using the local averaging in the non-homogeneous direction of the flow domain and by clipping the negative values of μ_{sgs}.

The present simulations have been carried out using 3D-PURLES which is based on a finite volume procedure (Rajani 2012) to solve the unsteady incompressible Navier Stokes equations in non-orthogonal curvilinear coordinates system with cartesian velocity. The code is based on SIMPLE algorithm (Patankar 1980), modified for collocated variable arrangement (Majumdar 1988) which uses central difference or other higher order upwind schemes for spatial discretisation and three-level fully implicit scheme for the temporal derivatives. The system of linear equations derived from the finite volume procedure is solved sequentially for the velocity components, pressure correction and turbulence scalars using the strongly implicit procedure of Stone (Stone 1968). The turbulent flow is modelled either by using URANS or LES approach. The algorithm is also parallelized using standard MPI routines.

3. RESULT AND DISCUSSION

3.1 Computational Details

The spatial resolution of the grid is usually decided by the length scales of the boundary layer on the cylinder surface, the separating free shear layers and the streamwise vortical structures in the wake. The details of the domain size, grid resolution and the numerical schemes used by other researchers for numerical simulation of flow past circular cylinder at $Re = 3900$ are given in Table 1 and 2 respectively.

Table 3 gives the overview of the different grid resolutions, domain size and models used for the present computation. The farfield location ($30D$) and the span length (πD) is fixed based on an earlier sensitivity study (Rajani 2012). The three-dimensional grid is generated by stacking equally in the spanwise direction (z/D) the two-dimensional radial polar grid obtained on the $z/D = 0$ plane. The different grids with varying circumferential and spanwise resolution are stretched in the radial direction so that the near wall-normal distance is maintained to be approximately $10^{-4}D$ in order to obtained the near wall y^+ to be less than one. Based on the boundary layer analysis, the boundary layer thickness (δ) for the finest grid (Run 6 and Run7) is estimated to be $0.0476D$ at $\theta = 80°$ on the cylinder which is covered by about 82 grid lines whereas, the δ for the coarse grid (Run 2, Run 4 and Run 5) is estimated to be $0.0485D$ at $\theta = 80°$ on the cylinder which is covered by about 55 grid lines. This analysis shows that the grid resolution used for the present LES computation at $Re = 3900$ is fine enough to resolve the boundary layer. The non-dimensional time step $\Delta\bar{t}$ ($= U_\infty \Delta t/D$) is fixed as 0.05 based on the preliminary sensitivity analysis carried out. An impulsive start of the cylinder is simulated by specifying uniform velocity at the inflow boundary, convective boundary condition at outflow boundary ($\frac{DU_k}{Dt} = 0$), no slip condition at cylinder wall boundary and perodic boundary in the spanwise direction.

Table 4 summarises the comparison between the present prediction and measurement (Cardell 1993; Lourenco and Shih 1993; Norberg 1987; Ong and Wallace 1996; Son and Hanratty 1969), data as well as other computational results for some of the important mean flow parameters like the drag coefficient ($\overline{C}_d$), base pressure coefficient ($-\overline{C}_{pb}$), recirculation length ($\frac{\overline{L}}{D}$), separation angle (θ_{sep}) and Strouhal number (St). The agreement between the present prediction of mean flow quantities and corresponding results from other sources is observed to be reasonably good for the LES computations using both the SGS models. Doubling of the grid size in all the direction for the SSM computations (Run 6) has slightly improved the mean quantities when compared to the SSM coarse grid computation (Run 5) The dynamic SGS model coupled to the fine grid (Run 7) predict the mean quantities closest to the measurement data but is not significantly different from the SSM results for fine grid (Run 6). The computations of 2D LES with no model (Run 1), the 2D URANS (Run 3) and 3D URANS (Run 4) grossly overpredict all the mean quantities as well and shedding frequency (St) and further they have even failed to capture the recirculation bubble. On the other hand, the 3D LES with no model has shown a better prediction but still is not in good agreement with the measurement data.

Table 1 Grid parameters used by other researchers at $Re = 3900$

Simulation [Reference]	Domain size $L_x \times L_y \times L_z$	Number of grid points	Time step size ($\Delta\bar{t}$)
LES Hansen and Long (2002)	$20D \times 10D \times 4D$	308,208 Tetra ($N_z = 28$)	-
LES Snyder and Degrez (2003)	$20D \times 7D \times \pi D$	23,500 Triangles ($N_z = 32$)	0.001
LES Kravchenko and Moin (2000)	$20D \times 20D \times \pi D$	$291 \times 258 \times 48$	-
LES (C2) of Breuer (1998)	$30D \times 30D \times \pi D$	$165 \times 165 \times 32$	-
LES (C3) of Breuer (1998)	$30D \times 30D \times \pi D$	$165 \times 165 \times 32$	-
LES (HR) Parnadeau *et al.* (2008)	$20D \times 20D \times \pi D$	$961 \times 960 \times 48$	0.003
LES Blackburn and Schmidt (2001)	$48D \times 7D \times \pi D$	1,474,560 Tretra ($N_z = 48$)	-
LES Franke and Frank (2002)	$20D \times 20D \times \pi D$	$193 \times 153 \times 33$	0.00264
LES (Case V) Ma *et al.* (2000)	$25D \times 18D \times 1.5\pi D$	-	-
DNS (Case II) Ma *et al.* (2000)	$25D \times 18D \times \pi D$	-	-
LES You and Moin (2006)	$50D \times 60D \times \pi D$	7,543,680 Tetra ($N_z = 65$)	-
LES Ouvrard et al. (2010)	$35D \times 40D \times \pi D$	1.46×10^6 Tetra	≈ 0.01

Table 2 Numerical models used by other researchers at $Re = 3900$

Simulation [Reference]	Numerical procedure	Discretisation scheme	SGS model	C_s	N_c
LES Hansen and Long	FV (UG)	CDS (2^{nd} order)	SSM	0.1	10
LES Snyder and Degrez	FES	Upwind	SSM	0.2	6
LES of Kravchenko and Moin	FES	B-Spline	DSM		20
LES Breuer	FV	CDS (2^{nd} order)	SSM	0.1	56
LES Breuer	FV	CDS (2^{nd} order)	DSM		56
LES Parnadeau *et al.*	IBM	CCDS (6^{th} order)	SFM		40-50
LES of Blackburn and Schmidt	FES	-	SSM	0.1	-
LES Franke and Frank	FV	CDS (2^{nd} order)	SSM	0.1	10 & 42
LES Ma *et al.*	FES (UG)	-	SSMP	0.196	131
DNS Ma *et al.*	FES (UG)	-	-	-	131
LES You and Moin	FV (UG)	2^{nd} order	DM1	-	-
LES & VMS-LES Ouvrard et al.	FVFEC (UG)	MUSCL (2^{nd} order)	WALE	-	25

Table 3 Grid parameters used for present computations

Run	Grid	Domain $L_x \times L_y \times L_z$	Model
Run 1 : 2D LES (CR)	120×145	$30D \times 30D$	No
Run 2 : 3D LES (CR)	$120 \times 145 \times 32$	$30D \times 30D \times \pi D$	No
Run 3 : 2D URANS (CR)	120×145	$30D \times 30D$	$k-\varepsilon$ of Chien (1982)
Run 4 : 3D URANS (CR)	$120 \times 145 \times 32$	$30D \times 30D \times \pi D$	$k-\varepsilon$ of Chien (1982)
Run 5 : 3D LES (CR)	$120 \times 145 \times 32$	$30D \times 30D \times \pi D$	SSM
Run 6 : 3D LES (HR)	$360 \times 242 \times 64$	$30D \times 30D \times \pi D$	SSM
Run 7 : 3D LES (HR)	$360 \times 242 \times 64$	$30D \times 30D \times \pi D$	DSM

3.2 Time Averaged Flow Field

The mean flow quantities and the mean turbulent stresses, obtained from the present LES computation for different grid resolutions and different models are compared with the corresponding measurement data of Norberg (1987), Lourenco and Shih (1993) and Ong and Wallace (1996) and shown in Fig. 1 to Fig. 7. The time averaged flow quantities have been obtained over approximately 20 vortex shedding cycles and the flow quantities are also averaged over the spanwise direction. In order to check the adequacy of the averaging sample size, the time averaged flow field for Run 6 was also obtained by doubling the sample size which did not bring any change in the values of the mean flow quantities and turbulent stresses.

Figure 1 shows the present prediction of the mean surface pressure coefficient (C_p) around the cylinder obtained for the different runs, compared to the measurement data of Norberg (1987). The agreement is observed to be rea-

Table 4 Computed mean flow quantities at $Re = 3900$

	$\overline{C}_d$	$-\overline{C}_{pb}$	St	$\overline{\theta}_{sep}$	$\frac{\overline{L}}{D}$	$\overline{U}_{\min}$
Present Computation						
Run 1	1.66	2.027	0.274	102°	-	-
Run 2	1.15	1.068	0.195	90°	1.057	-0.28
Run 3	1.65	2.019	0.244	102°	-	-
Run 4	1.27	1.511	0.225	98°	0.305	-0.09
Run 5	1.10	0.947	0.200	88°	1.010	-0.29
Run 6	1.05	0.928	0.214	87.5°	1.211	-0.27
Run 7	1.01	0.900	0.210	87.5°	1.198	-0.28
Other References						
LES of Hansen and Long (2002)	1.31	1.339	0.207	-	0.732	-0.26
LES of Snyder and Degrez (2003)	1.09	-	0.2	88°	1.300	-0.29
LES of Kravchenko and Moin (2000)	1.04	0.940	0.210	88°	1.350	-0.37
LES (C2) of Breuer (1998)	1.10	1.047	-	87.9°	1.115	-
LES (C3) of Breuer (1998)	1.07	1.011	-	87.7°	1.197	-
LES (HR) of Parnadeau *et al.* (2008)	-	-	0.208	-	1.560	-0.26
LES of Blackburn and Schmidt (2001)	1.01	0.930	0.218	-	-	-
LES ($N_c = 10$) of Franke and Frank (2002)	1.01	0.940	0.209	89°	1.340	-
LES ($N_c = 42$) of Franke and Frank (2002)	0.98	0.850	0.209	88.2°	1.640	-
LES (Case V) of Ma *et al.* (2000)	-	0.765	0.208	-	1.760	-
DNS (Case II) of Ma *et al.* (2000)	-	0.840	0.219	-	1.590	-
LES DM of (Park *et al.* 2006)	1.04	0.94	0.212	-	1.37	-
LES DM1 of (You and Moin 2006)	1.01	0.92	0.224	-	-	-
LES WALE of (Ouvrard et al. 2010)	1.02	0.94	0.221	-	1.22	-
VMS-LES WALE of (Ouvrard et al. 2010)	0.94	0.83	0.223	-	1.56	-
Measurements	0.98	0.88	0.215	86°	1.3	−0.25
	±0.05	±0.05	±0.005	±2	±0.1	±0.1

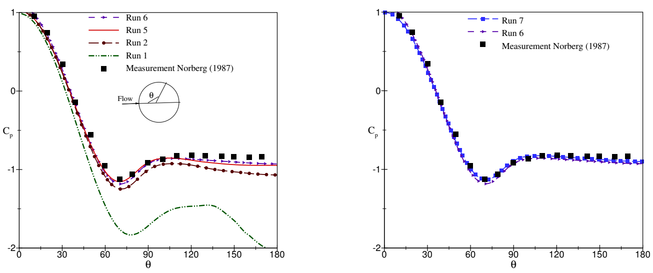

(a) Variation of Runs (Table 3) (b) Effect of SGS model

Fig. 1. Comparison of the computed surface pressure coefficient distribution.

sonably good for the accelerating flow part beyond the stagnation point and also for the suction peak ($C_{p_{\min}} = -1.16$). The effect of grid refinement from Run 5 to Run 6 and effect of SGS models (Run 6 and Run 7) was observed to bring in an insignificant improvement in the mean value of the base pressure coefficient. The pressure coefficient obtained from the 2D LES with no model (Run 1) completely differs from the measurement and the other runs (Fig. 1(a)). However, the 3D LES with no model (Run 2) has captured the pressure coefficient reasonably well but has slightly overpredicted the suction peak and the base pressure coefficient. In spite, of minor discrepancies amongst different LES runs (Run 5 to Run 7), the predicted base pressure ($-C_{pb} = 0.900$) with the finest grid resolution coupled to dynamic SGS model (Run 7) is the closest to the measurement data ($-C_{pb} = 0.88 \pm 0.05$) as shown in Fig. 1(b) and Table 4. The same is observed for the mean drag coefficient (C_d) and other mean parameters.

The longitudinal variation of the mean streamwise velocity along the wake centerline (U_{CL}), shown in Fig. 2, indicates a fairly good agree-

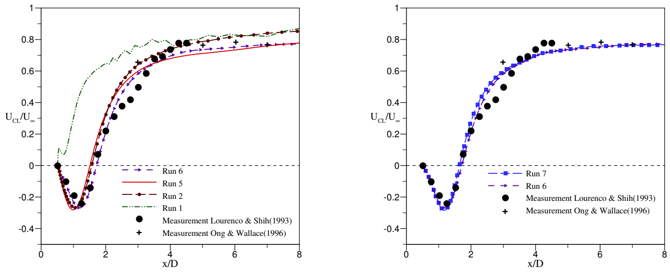

(c) Variation of Runs (Table 3) (d) Effect of SGS

Fig. 2. Comparison of mean streamwise velocity along wake centerline.

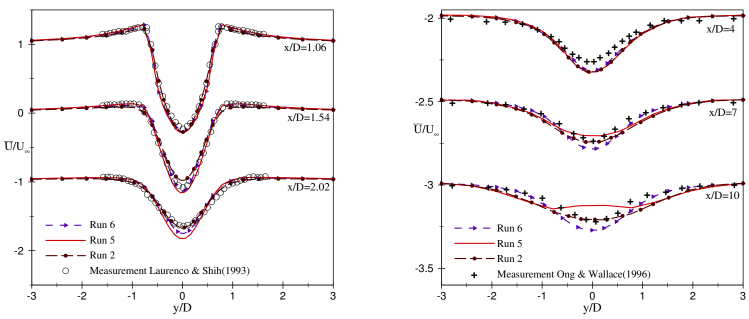

(e) Effect of grid size

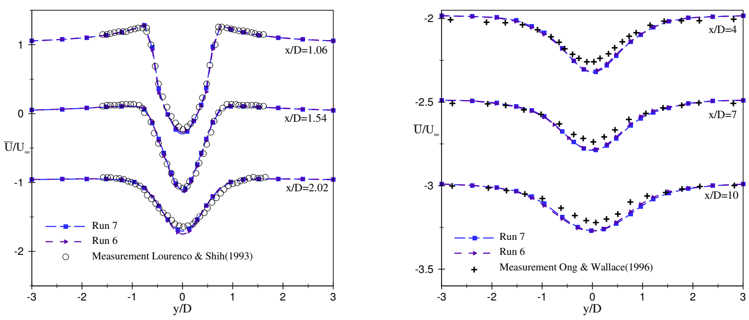

(f) Effect of SGS model

Fig. 3. Comparison of transverse profiles of mean streamwise velocity.

ment between measurement of Lourenco and Shih (1993) and the present LES computations. The recirculation bubble length has been captured reasonably well by all 3D LES runs. However as mentioned earlier the 2D LES with no model has failed to capture the recirculation bubble as clearly indicated in Fig. 2(a). The fine grid results obtained from the two SGS models are almost identical with Run 7 being closest to the measurement data (Fig. 2(b)). The minimum negative streamwise velocity ($U_{\min}$ in Table 4) inside the recirculation zone which indicates the strength of the Karman vortices is predicted quite accurately by the 3D LES. However, in the far wake ($x/D > 4$), some discrepancies are observed which may be attributed partly to the discretisation error as discussed in details by Ghosal (1996) and partly to the numerical diffusion caused by use of a relatively coarser grid in the far wake of the cylinder.

The transverse profiles of mean velocity and turbulent Reynolds stress components of the present LES computation are compared to the corresponding PIV data of Lourenco and Shih (1993) in the near wake ($x/D \leq 2.02$) and the hot wire measurement data of Ong and Wallace (1996) in the far wake ($4 \leq x/D \leq 10$). Figure 3 shows the mean streamwise velocity profiles ($\overline{U}/U_\infty^2$) at six different longitudinal stations between $x/D = 1$ and 10. In the near wake ($x/D \leq 2$), the agreement between the measurement data and the present LES compu-

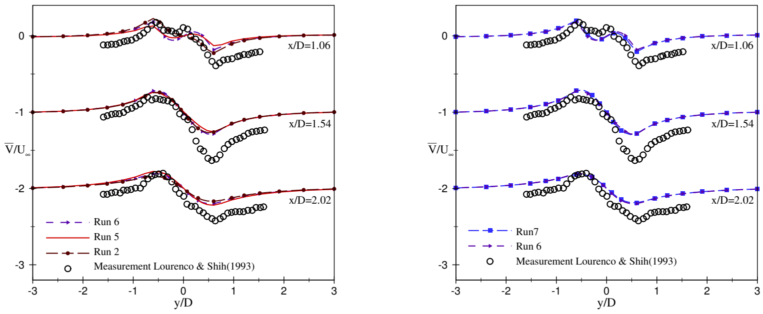

(g) Effect of grid size (h) Effect of SGS model

Fig. 4. Comparison of transverse profiles of mean cross-stream velocity.

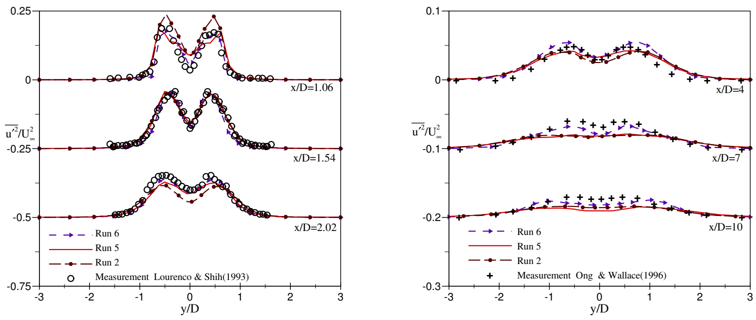

(i) Effect of grid size

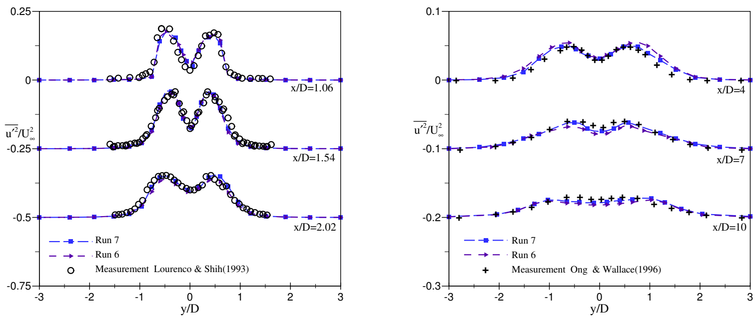

(j) Effect of SGS model

Fig. 5. Transverse profiles of the streamwise component of the resolved mean turbulent stress.

tation with different grid resolutions (Run 5 and Run 6) and SGS models (Run 2, Run 6 and Run 7) is reasonably good. The present LES computation has predicted a higher velocity at $x/D = 4$ near the wake centerline region when compared to the measurement data may be attributed to the difference is recirculation length (Fig. 2). However the profile at $x/D = 4$ is in similar to that obtained by the DNS data of Ma *et al.* (2000). On the other hand, in the far wake region ($x/D > 4$), the trend of variation of the mean velocity with a single dip near the wake centerline is captured by all runs in general; but the quantitative agreement is observed to be best for LES with SSM and DSM using the finest resolution (Run 6 and Run 7).

The transverse profiles of mean cross-flow velocity component ($\overline{V}/U_\infty^2$) at three different near wake stations are shown in Fig. 4. Though the trends are correct, major discrepancies are observed in the maximum magnitude of the cross-flow velocity component. Similar discrepancies have also been observed in LES computation of

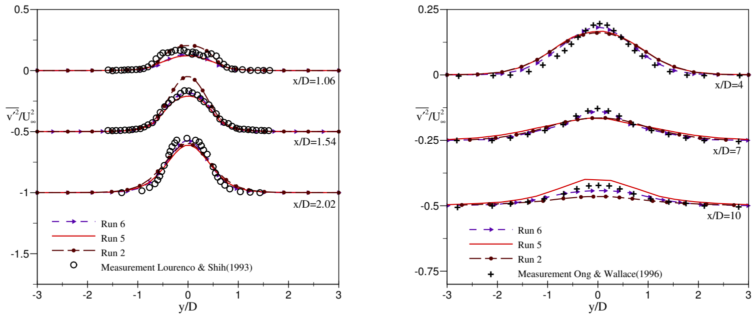

(k) Effect of grid size

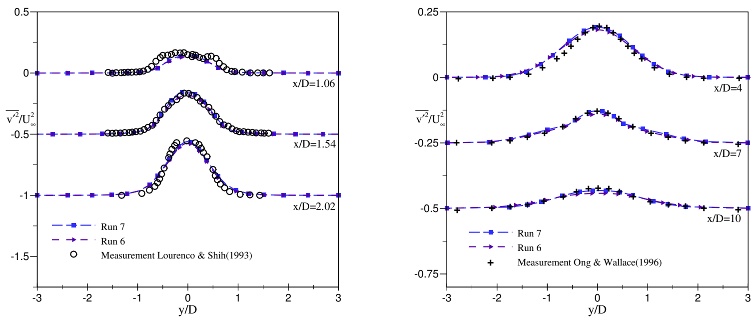

(l) Effect of SGS model

Fig. 6. Transverse profiles of the cross-flow component of the resolved turbulent stress.

the same flow situation reported by earlier researchers (Kravchenko and Moin 2000; Franke and Frank 2002; Ma *et al.* 2000).

Figure 5 and Figure 6 show the profiles of the time averaged streamwise and cross-flow components of the resolved turbulent normal stresses respectively at six different longitudinal stations. Differences are observed in the profiles obtained by different runs (Run 2, Run 5 and Run 6) right from the first station. However these profile obtained for the fine grid computation using SSM (Run 6) and DSM (Run 7) are more or less similar and closer to the measurement data. Upto $x/D = 4$ a good agreement is achieved between measurement of Lourenco and Shih (1993) and fine grid predictions (Run 6 and Run 7) for both the streamwise, $\overline{u'^2}/U_\infty^2$ (Fig. 5) and cross-flow, $\overline{v'^2}/U_\infty^2$ (Fig. 6) components of the resolved turbulent normal stress. In the far wake stations, the double peak of the stress component around the flow axis is captured only by the fine grid computation (Run 6 and Run 7) but its magnitude is underpredicted with Run 7 (LES with DSM) being the closest to the measurement data. On the other hand, Run 2 and Run 5 have failed to capture the double peak as well its magnitude. Also, in case of cross flow component of the turbulent stress, especially in the downstream stations ($x/D \geq 4$),the agreement between the prediction and measurement data is observed to be the best for the Run 7. The Discrepancies observed in the profiles at the farwake locations may possibly be attributed to the relatively coarse grid size in the far wake zone where the radial dimension of the wedge shaped control volumes are large due to the stretching towards the cylinder surface. Even in case of Reynolds shear stress ($\overline{u'v'}/U_\infty^2$) component profiles, shown in Fig. 7, the agreement between the present prediction and the measurement data of Lourenco and Shih (1993) is observed to be good at all the stations for the fine grid computation *viz.* Run 6 and Run 7. All the runs have produced almost identical $\overline{u'v'}/U_\infty^2$ profiles up to $x/D = 4$ after which the coarse grid LES with no model and SSM (Run2 and Run5) is observed to deviate quite significantly.

3.3 Instantaneous Flow Fields

The contours of instantaneous vorticity magnitude zoomed near the cylinder surface in the $x-y$ plane obtained by Run 6 (fine grid SSM) and Run 7 (fine grid DSM) are shown in Fig. 8. The small scale flow structure in the wake region could be caputed only by fine grid compu-

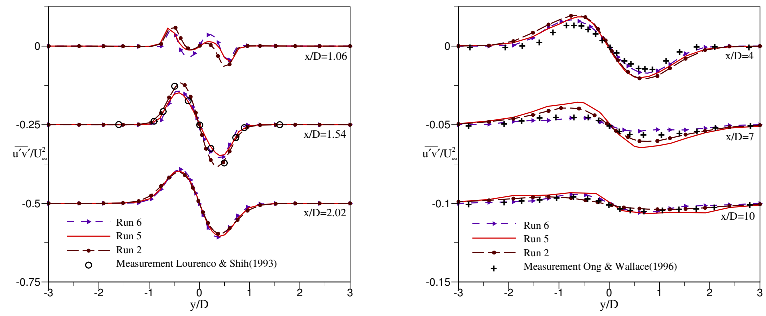

(m) Effect of grid size

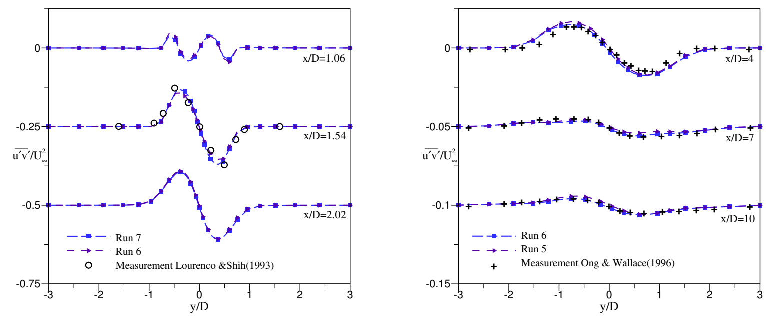

(n) Effect of SGS model

Fig. 7. Comparison of transverse profiles of mean Reynolds shear stress component.

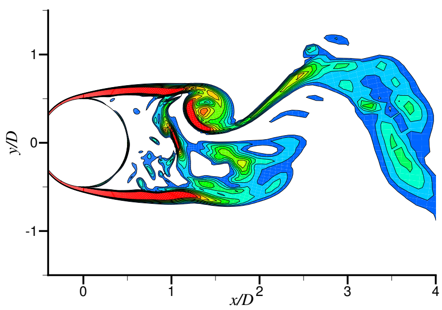

(a) Smagorinsky SGS model (Run 6 - Table 3)

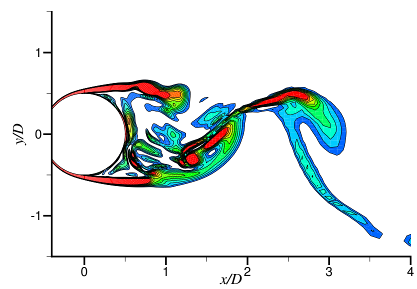

(b) Dynamic SGS model (Run 7 - Table 3)

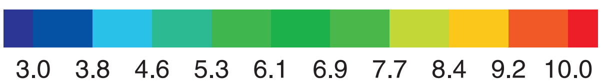

Fig. 8. Instantaneous vorticity magnitude ($|\,\omega\,|\, D/U_\infty$) - 10 contours from 3 to 10.0.

tation using both the SGS models. The Karman vortex street and the two long separating shear layers on both sides of the cylinder are clearly observed in the figure. Both the SGS model predict almost similar shear layer length thus indicating the transition to turbulence in the separated shear layer occurs around the same location for both the models. The breakdown of the shear layer is also clearly evident in this contour plot. A distinct feature of the flow at $Re = 3900$ is the longitudinal measure of the separating shear layer of about one diameter which has also been reported in the experimental studies (Prasad and Williamson 1997; Cardell 1993; Chyu and Rockwell 1996).

In the turbulent shear flow, the turbulent structures are often found to be dominated by ed-

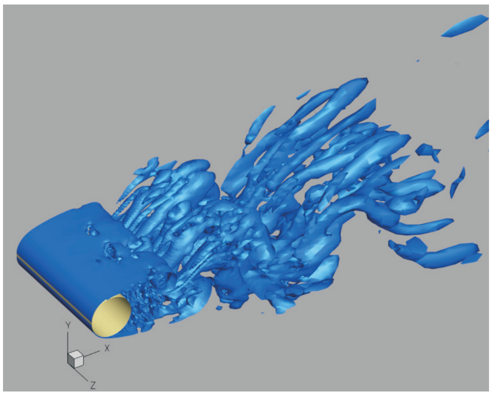

(d) Smagorinsky SGS model (Run 6 - Table 3)

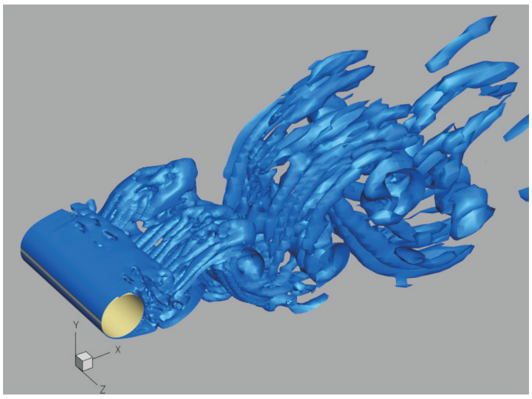

(e) Dynamic SGS model (Run 6 - 3)

Fig. 9. Instantaneous Q isosurfaces, $Q = 0.5$ at $Re = 3900$.

dies which preserve a certain spatially organisation and these vortical structures evolve temporally and there are many methods to identify and visualize these turbulent struture. Q-criteria $\left(Q = \frac{1}{2}\left(|\Omega|^2 - |S|^2\right)\right)$ proposed by Hunt *et al.* (1988) has been successfully used to identify vortices in the incompressible flows. Q represents the local balance between shear strain rate and vorticity magnitude. The positive Q isosurfaces isolate areas where the strength of rotation overcomes the strain rate and Q remains positive at the core of the vortex. The instantaneous isosurfaces of $Q = 0.5$ computed from the instantaneous velocity field of the fine grid computation using Smagorinsky and dynamic SGS models are shown in Fig. 9. The Q isosurfaces obtained by the two SGS models clearly give a clear visual impression of the vortical flow structures in the wake and its three-dimensional character. Further the breakup of the shear layer and the organisation of the chaotic turbulent eddies into a vortex street is also clearly evident.

4. Concluding Remarks

Numerical simulations of flow past a circular cylinder in the subcritical regime at $Re = 3900$ have been carried using LES with Smagorinsky SGS model (SSM) and dynamic SGS (DSM) model. In order to resolve the wide range of scales of the flow structure along the radial, streamwise and spanwise direction, different spatial resolutions have been used for the present LES computation with the finest grid size being $360 \times 242 \times 64$ (5.56 million control volumes). Agreement between the predictions and measurement data for the mean flow parameters like drag coefficient, base pressure, separation angle *etc.* as well as for velocity components and the resolved Reynolds stress components close to the cylinder ($X/D \leq 4$) confirms the accuracy and adequacy of the present LES algorithm coupled to two different SGS models as well as the grid resolution. Doubling of the grid size has improved the profiles of the mean flow quantities only in the far downstream location ($x/D \geq 7$) whereas for the mean turbulent stress profiles the improvement is observed in the near wake region itself ($x/D \geq 2.02$). Discrepancies between LES results and measurement data in the far wake especially for the streamwise and normal components of the resolved turbulent stress may be attributed to the use of relatively coarser grid size at far field zone due to the near wall stretching of radial polar grid lines towards the cylinder wall. In general, the LES results obtained using the dynamic SGS model are observed to have better agreement with the measurement data for both the mean and turbulent fluctuating quantities. However, the influence of SGS model on the overall results was found to be small and the merits of the dynamic SGS model over Smagorinsky SGS model could to be established in the present study. The vortical coherent structure and wake characteristics are captured reasonably well by the present LES simulation thus demonstrating its effectiveness and potential in handling bluff body problems and vortex dominated flows.

Acknowledgments

The authors wish to thank Director CSIR-NAL Bangalore for permitting us to publish this paper. Our heartfelt thanks to Dr. V. Y. Mudkavi Head, CTFD Division, CSIR-NAL Bangalore for his support and technical suggestions. Special thanks to Prof. Gautam Biswas, Dept. of Mechanical Engg., IIT Kanpur, India for his guidance during the implementation of the dynamic subgrid scale model.

REFERENCES

Beaudan, P. and Moin, P. (1994). *Numerical experiments on the flow past a circular at a sub-critical Reynolds number*. Report number TF62,Thermosciences Division, Department of Mechanical Engineering, Stanford University, 1–44.

Blackburn, H. M. and Schmidt, S. (2001). Large eddy simulation of flow past a circular cylinder. *Proceedings* 14^{th} *Australasia Fluid Mechanics Conference.* Adelaide University, Australia, 10–14 December.

Breuer, M. (1998). Numerical and modeling influence on Large Eddy Simulation for flow past circular cylinder. *International Journal of Heat and Fluid Flow* 19, 512–521.

Cardell, G. S. (1993). *Flow past a circular cylinder with a permeable splitter plate*. Ph.D Thesis, Graduate Aeronautical Lab., California Inst. of Technology.

Chien, K. Y. (1982). Predictions of channel and boundary layer flows with a low Reynolds no. turbulence model. *AIAA Journal* 20, 321–339.

Chyu, C. K. and Rockwell, D. (1996). Near-wake structures of an oscillating cylinder: Effect of controlled shear-layer vortices. *Journal of Fluid Mechanics* 322, 21.

Cox, J. S. (1997). *Computation of sound generated by viscous flow over a circular cylinder*. NASA TM 110339.

Deng, G. B., Piquet, J., Queutey, P. and Visonneau, M. (1993). Vortex-shedding flow prediction with eddy-viscosity models. Engineering Turbulence *Modelling and Experiments*, Elsevier Science, Amsterdam, 2, 143–152.

Dong, S., Karniadakis, G. E., Ekmekci, A. and Rockwell, D. (2006). A combined direct numerical simulation-particle image velocimetry study of the turbulent near wake. *Journal of Fluid Mechanics* 569, 185–207.

Franke, J. and Frank, W. (2002). Large eddy simulation of flow past a circular cylinder at Re_D=3900. *Journal of Wind Engineering and Industrial Aerodynamics* 90, 1191–1206.

Germano, M., Piomelli, U., Moin, P. and Cabot, W. (1991). A dynamic sub-scale eddy viscosity model. *Physics of Fluids A, 3(7)* 1760–1765.

Ghosal, S. (1996). An analysis of numerical errors in large-eddy simulation of turbulence. *Journal of Computational Physics* 125, 187–206.

Hansen, R. P. and Long, L. N. (2002). Large-eddy simulation of a circular cylinder on unstructured grids. 40^{th} *AIAA Aerospace Sciences Meeting and Exhibit* 14-17 January, Reno, NV, 2002-0982, 1–11.

Hunt, J. C. R., Wray, A. A. and Moin, P. (1988). *Eddies, stream, and convergence zones in turbulent flows*. Center for Turbulence Research Report, CTR-S88, 193–208.

Kravchenko, A. G. and Moin, P. (2000). Numerical studies of flow over a circular cylinder at $Re_D = 3900$. *Physics of Fluids* 12 (2), 403–417.

Lilly, D. K. (1992). A proposed modification of the Germano sub grid scale closure method. *Physics of Fluids A* 4, 633–635.

Lourenco, L. M. and Shih, C. (1993). *Characteristics or the plane turbulent near wake of a circular cylinder, a particle image velocimetry study*. Published in Beaudan and Moin(1994),data taken from Kravchenko and Moin(2000).

Ma, X., Karamonos, G. S. and Karniadakis, G. E. (2000). Dynamics of low-dimensionality of a turbulent near wake. *Journal of Fluid Mechanics* 410, 29–65.

Majumdar, S. (1988). Role of underrelaxation in momentum interpolation for calculation of flow with non-staggered grids. *Numerical Heat Transfer* 13, 125–132.

Mittal, R. and Balachandra, S. (1997). On the inclusion of three-dimensional effects in simulation of two-dimensional bluff-body wake flows. *ASME Fluids Engineering Division Summer Meeting* , 1–6.

Mittal, R. and Moin, P. (1997). Suitability of upwind-biased finite-difference schemes for large eddy simulation of turbulent flow . *AIAA journal* 35, 1415–1417.

Mittal, S. (2001). Computation of three dimensional flow past circular cylinder of low aspect ratio. *Physics of Fluids* 13, 177–191.

Najjar, F. M. and Tafti, D. K. (1996). Study if discrete test filters and finite difference approximations for the dynamic sub grid-scale model. *Physics of Fluids* 8(4), 1076–1088.

Nicoud, F. and Ducros, F. (1999). Subgrid-scale stress modelling based on the square of the velocity gradient tensor . *Flow Turbulence Combustion* 62(3), 183–200.

Norberg, C. (1987). *Effects of Reynolds number and a low- intensity free-stream turbulence on the flow around circular cylinder*. Publication No. 87/2, Department of Applied Thermodynamics and Fluid Mechanics, Chalmers University of Technology, Sweden.

Ong, L. and Wallace, J. (1996). The velocity field of the turbulent very near wake of a circular cylinder. *Experiments in Fluids* 20, 441–453.

Ouvrard, H., Koobus, B., Camarri, S., Dervieux, A. and Salvetti, M. V. (2010). Classical and variational multiscale LES of the flow around a circular cylinder on unstructured grids . *Computers and Fluids* 39(7), 1083–1094.

Park, N., Lee, S., Lee, J. and Choi, H. (2006). A dynamic subgrid-scale eddy viscosity model with a global model coefficient. *Physics of Fluids* 18(2), 125109.

Parnadeau, P., Carleir, J. and Lamballais, E. (2008). Experimental and numerical studies of the flow over a circular cylinder Reynolds number 3900. *Physics of Fluids* 20(8), 1–14.

Patankar, S. V. (1980). Numerical heat transfer and fluid flow, Hemisphere Pub. Co.

Prasad, A. and Williamson, C. H. K. (1997). The instability of the shear layer separating from a bluff body. *Journal of Fluid Mechanics* 333, 375.

Rai, M. M. and Moin, P. (1993). Direct numerical simulation of transition and turbulence in a spatially evolving boundary layer . *Journal of Computational Physics* 109, 169.

Rai, M. M. (2010). A computational investigation of the instability of the detached shear layer in the wake of a circular cylinder. *Journal of Fluid Mechanics* 659, 375–404.

Rajani, B. N. (2012). *Numerical simulation of flow around a circular cylinder*. Ph. D. thesis, National Institute of Technology Karnataka.

Rajani, B. N., Kandasamy, A. and Majumdar, S. (2009). Numerical simulation of laminar flow past a circular cylinder. *Applied Mathematical Modelling* 33, 1228–1247.

Rajani, B. N., Kandasamy, A. and Majumdar, S. (2012). Limitations of URANS simulation for prediction of two-dimensional turbulent flow past a circular cylinder. *Journal of Applied Fluid Mechanics* 5, 67–79.

Roshko, A. (1954). *On the development turbulence wakes from vortex streets*. NACA Report 1191.

Sagaut, P. (1998). *Large-eddy simulation for a incompressible flows - An introduction*, Springer.

Smagorinsky, J. (1963). General circulation experiments with the primitive equation.I:The basic experiment. *Monthly Weather Review* 91, 99–163.

Snyder, D. O. and Degrez, G. (2003). Large-eddy simulation with complex 2-D geometries using a parallel finite element/spectral algorithm. *International Journal for Numerical Methods in Fluids* 41, 1119–1135.

Son, J. and Hanratty, T. J. (1969). Velocity gradients at the wall for flow around a cylinder at Reynolds number from 5×10^3 to 10^5. *Journal of Fluid Mechanics* 35, 353–368.

Stone, H. L. (1968). Iterative solution of implicit approximations of multidimensional partial differential equations. *SIAM Journal of Numerical Analysis* 5, 530–530.

Thompson, M., Hourigan, K. and Sheridan, J. (1996). Three dimensional instabilities in the wake of a circular cylinder. *Experimental & Thermal Fluid Science* 12, 190–196.

Vreman, A. W. (2004). An eddy-viscosity subgrid-scale model for turbulent shear flow : algebraic theory and application . *Physics of Fluids* 16(10), 3670–3681.

Williamson, C. H. K. (1996). Vortex dynamics in the cylinder wakes. *Annual Review of Fluid Mechanics* 28, 477–539.

Wissink, J. G. and Rodi, W. (2008). Numerical study of the near wake of a circular cylinder' . *International Journal of Heat and Fluid Flow* 29, 1060–1070.

You, D. and Moin, P. (2006). *A dynamic global-coefficient subgrid-scale eddy-viscosity model for large-eddy simulation in complex geometries*. Annual

Research Briefs, Center for Turbulence Research, 41–53.

Zang, Y., Street, R. L. and Koseff, R. (1993). A dynamic mixed sub grid-scale model and its application to turbulent recirculating flows. *Physics of Fluids A* 5(12), 3186–3196.

Zdravkovich, M. (1997). *Flow around circular cylinders:* V.1, Oxford Science Publication.

Zhang, H. Q., Fey, U., Noack, B. R., König, M. and Eckelmann, H. (1995). On the transition of the cylinder wake. *Physics of Fluids* 7, 779–794.